APPLICATION OF BOREHOLE-RADAR METHODS TO IMAGE TWO PERMEABLE REACTIVE-IRON WALLS AT THE MASSACHUSETTS MILITARY RESERVATION, CAPE COD, MASSACHUSETTS

Peter K. Joesten, U.S. Geological Survey, Storrs, CT
John W. Lane, Jr., U.S. Geological Survey, Storrs, CT
Jennifer G. Savoie, U.S. Geological Survey, Northborough, MA
Roelof J. Versteeg, Columbia University, New York, NY

Abstract

A pilot-scale study was conducted at the Massachusetts Military Reservation, Cape Cod, Massachusetts, to assess the use of a hydraulic-fracturing method to create vertical permeable walls of zero-valent iron to remediate ground water contaminated with chlorinated solvents at depths exceeding the range of conventional iron-wall installation methods. At the test site, ground-water contamination extends from 24 to 37 meters (m) below land surface. A treatment zone consisting of two parallel reactive-iron walls 12 m long, 13 m high, and 0.15 m thick, separated by about 6 m, was designed to intersect and remediate a portion of the CS-10 plume. The U.S. Geological Survey used a cross-hole, common-depth radar scanning method to test the continuity and estimate the lateral and vertical extent of the two reactive-iron walls. The cross-hole radar surveys were conducted in boreholes on opposite sides of the iron injection zones. Significant decreases in the amplitude of the radar pulse observed in scans traversing the injection zones were interpreted by comparing radar field data to results of two-dimensional, finite-difference, time-domain models and laboratory-scale physical models developed to predict the effects of wall edges and discontinuities on common-depth cross-hole radar measurements. As part of a feasibility study, single-hole radar reflection data was used successfully to image the walls.

Introduction

Ground water beneath and downgradient from the Massachusetts Military Reservation (MMR), on Cape Cod, Massachusetts, has been affected by various contaminants, including chlorinated solvents, used during past decades of military operations. Chlorinated solvents that have entered the ground-water system are moving away from the MMR in the underlying sand-and-gravel aquifer toward streams, ponds, and coastal bays (fig. 1) (ABB Environmental Services, Inc., 1993).

In an attempt to prevent continued spread of these chemicals from the source area, a pilot-scale permeable zero-valent iron remediation system was installed in the Chemical Spill 10 (CS-10) plume. Zero-valent iron has been used to remediate ground water contaminated with chlorinated solvents (Gillham and O'Hannesin, 1994) at several sites in North America and Europe. As contaminated ground water moves through the treatment zone, chlorinated solvents are reductively dechlorinated to less harmful chemicals (Gillham and O'Hannesin, 1994).

At the test site, the CS-10 plume is located from 24 to 37 meters (m) below land surface. This exceeds the practical installation limits of the funnel-and-gate design, which is commonly used for permeable zero-valent iron remediation systems (Starr and Cherry, 1994; Smyth and others, 1996). The installation method selected for the CS-10 plume was hydraulic fracturing (Hubble and Gillham, 1997; Hubble and Gillham, 1999). The hydraulic-fracturing method uses a proprietary injection technology to inject a permeable barrier of zero-valent iron in unconsolidated sediments (G. Hocking

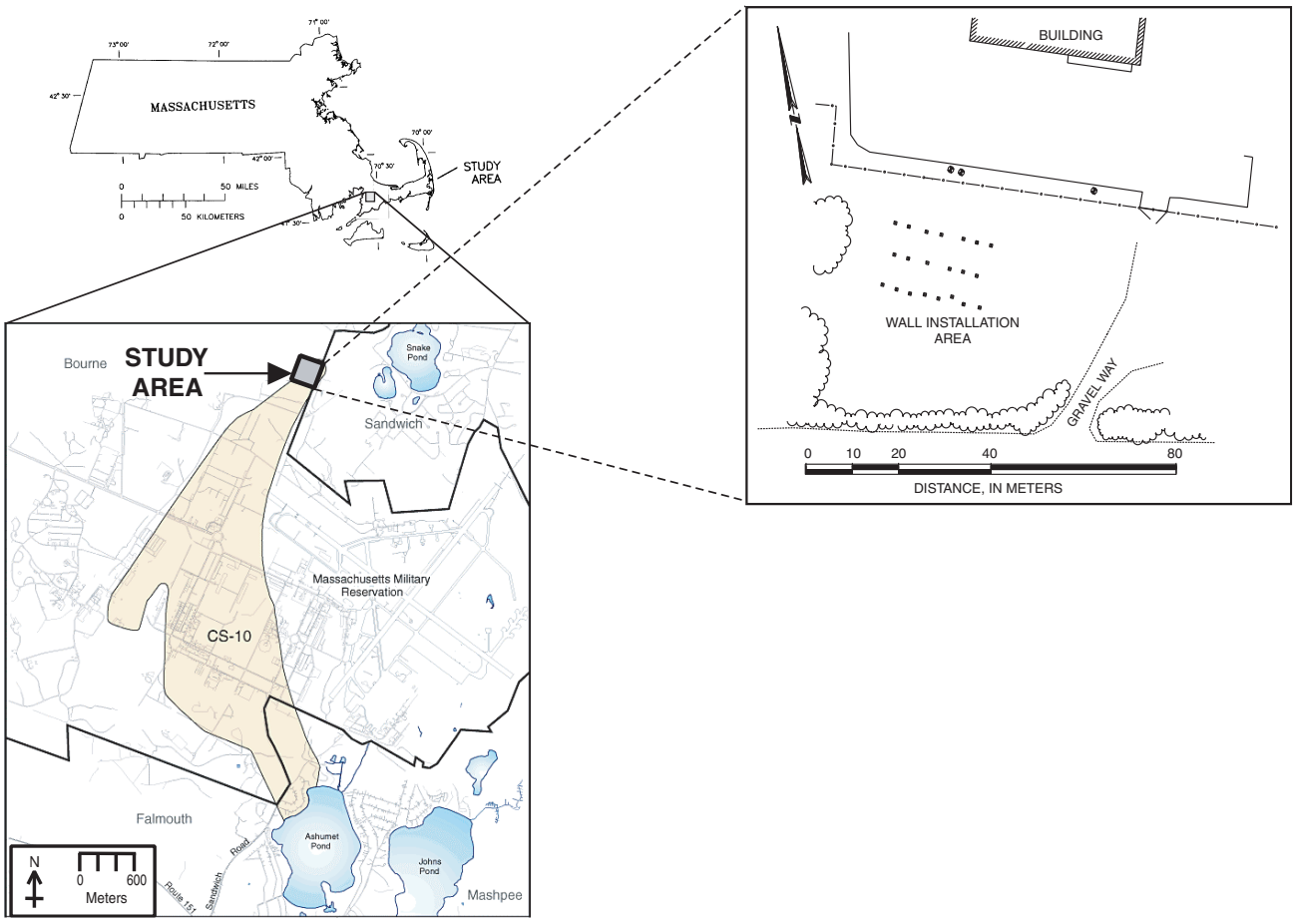

Figure 1. Location of the study area and the CS-10 plume, Massachusetts Military Reservation, Cape Cod, Massachusetts.

and S.L. Wells, Golder Sierra LLC, written commun., 1997). In 1998 a pilot-scale test of the installation method was conducted near the source area of the CS-10 plume in which two parallel vertical iron walls, 12 m long, 13 m high, and 0.15 m thick, were designed to intersect the contaminated ground water. The pilot-scale test was intended to demonstrate the application of the in-place remediation technology and the vertical hydraulic-fracturing method of installation.

The depth of the installation prevented physical inspection of the walls; therefore a remote-sensing method was required to determine the boundaries and continuity of the walls. In 1998 a study was conducted using common-depth (CD) cross-hole radar scanning as a remote-sensing method to determine the lateral and vertical extent of the iron walls and to determine whether large holes that could allow contaminated ground water to pass untreated through the remediation zone were present in the iron walls. The cross-hole radar method was chosen because a radar pulse can be significantly absorbed by accumulations of iron particles between a radar transmitter and receiver. To constrain the estimates of wall boundaries and continuity, the effect of wall edges and holes on the cross-hole radar data was predicted through numerical and physical modeling. Single-hole radar reflection surveys were also conducted to image the walls.

Numerical and Physical Modeling

For this study the wall-construction materials and vertical-emplacement geometry imposed constraints on the use of conventional tomographic-imaging methods. Because the iron used in the

construction of the walls was expected to absorb the radar waves, large regions of the iron injection zones were expected to act as perfect conductors that would completely block directly transmitted radar pulses. Perfect conductors are opaque to the radar; therefore many of the measurements used for tomography are eliminated, degrading the quality, resolution, and uniqueness of tomograms produced from the cross-hole radar data.

The use of the perfect conductor conceptual model reduces the imaging problem to the identification of (1) conductor edges and (2) holes within the conductor. This simplifies cross-hole radar data acquisition by limiting measurements to horizontal scans acquired from radar transmitters and receivers located at common depths. Instead of using conventional tomographic-image reconstruction methods, radar field data were analyzed using the results of numerical and physical models developed to predict the effects of wall edges and discontinuities on CD cross-hole radar measurements.

Numerical Modeling

For this study, the effect of wall edges and holes on CD cross-hole radar amplitudes was modeled using a two-dimensional, finite-difference time-domain (2-D FDTD) numerical code (Xiao and others, 1998). The finite-difference grid for the numerical models contained 5-centimeter (cm) by 5-cm cells, and the model domain extended 12.8 m (256 cells) in both the horizontal and vertical directions (fig. 2). The outer 2.5 m (50 cells) of the model domain is a super-absorbing boundary to minimize model-boundary reflection effects (Xiao and others, 1998). The electromagnetic properties of simulated materials within the model domain were consistent with field measurements at the site. The models simulated saturated sand with a relative dielectric permittivity of 25, an electrical conductivity of 0.01 Siemens per meter, and a relative magnetic permeability of 1. Because the electrical conductivity of iron is so high, the model wall was approximated as a near-perfect conductor with a thickness of 10 cm. The cross-hole radar pulse was simulated using a Ricker wavelet (Ricker, 1953) that had a frequency of 250-megahertz (MHz) and a wavelength in saturated sand of 24 cm. Time-domain waveforms produced by the numerical models were sampled at 5,270 MHz using 1,024 samples per waveform.

In the modeling, the CD radar scans were simulated by moving the transmitter and receiver locations in 10-cm intervals along the model boundaries parallel to the simulated walls. The horizontal separation between the radar transmitter and receiver ranged from 5.00 to 7.25 m to simulate the distances between boreholes at the field site.

The first model contained a 10-cm thick vertical wall that extended from the center of the model domain to the lower model boundary was used to determine the effect of wall edges on the directly transmitted cross-hole radar pulse (fig. 2a). Radar-pulse amplitudes from the edge models are plotted against position relative to the top of the wall in figure 3. The modeled pulse amplitudes were normalized to an average background pulse amplitude obtained from a model without a wall. For the range of horizontal transmitter-receiver separations in this study, when the modeled CD scan was at the edge of the wall, the simulated radar-pulse amplitude decreased to about 0.43 of the normalized background wave amplitude.

A second model that contained a 10-cm thick vertical wall extending across the model domain with a hole in the center was used to determine the effect of holes on the directly transmitted radar pulse (fig. 2b). The model simulated the effect of a hole in an iron wall over a range in hole apertures of 0 to 1.67 wavelengths (0 to 40 cm). Radar-pulse direct-wave amplitudes from the hole models are shown in figure 4. Based on the modeling, holes with a diameter of less than 40 percent of the wavelength of the radar pulse are not likely to be detected.

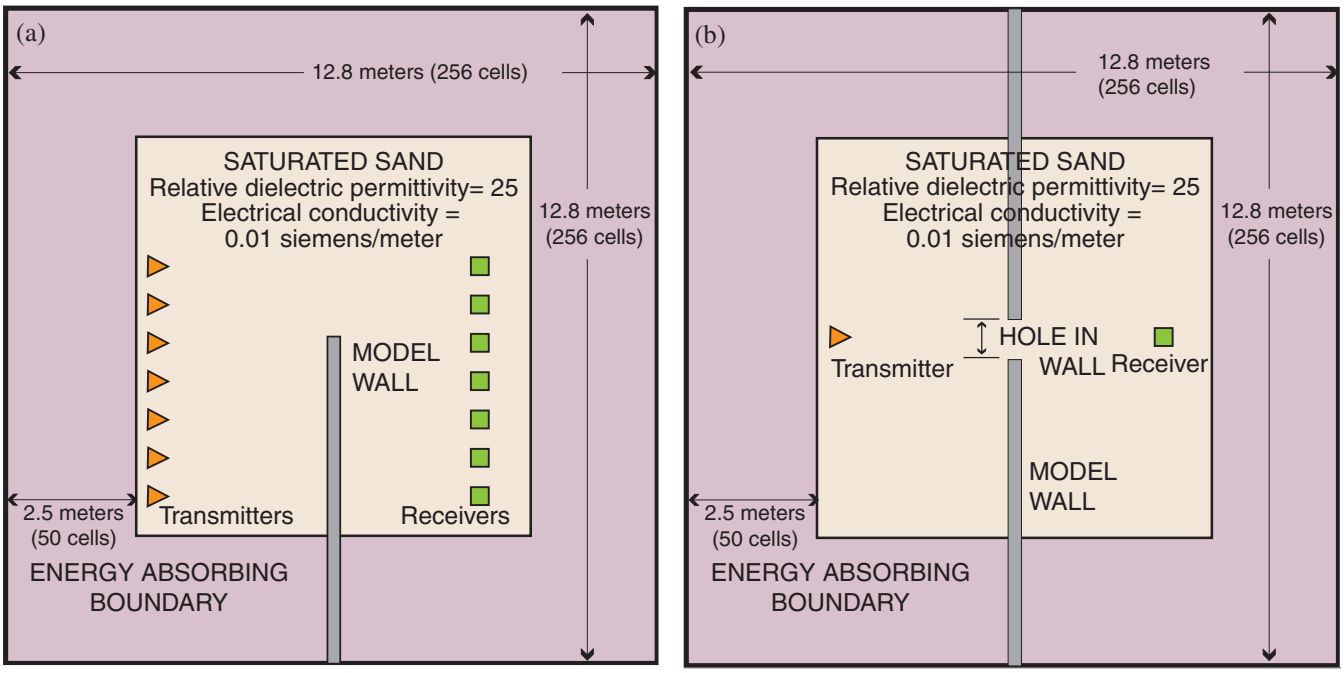

Figure 2. The finite-difference numerical model extending 12.8 meters (256 cells) in the vertical direction and 12.8 meters (256 cells) in the horizontal direction with (a) a wall extending from the center to the edge of the model to determine the effect of wall edges, and (b) a wall extending across the model with a hole in the center to determine the effect of a hole in the wall. There is a 2.5-m (50 cell) energy absorbing boundary on the edges of the model to minimize edge effects.

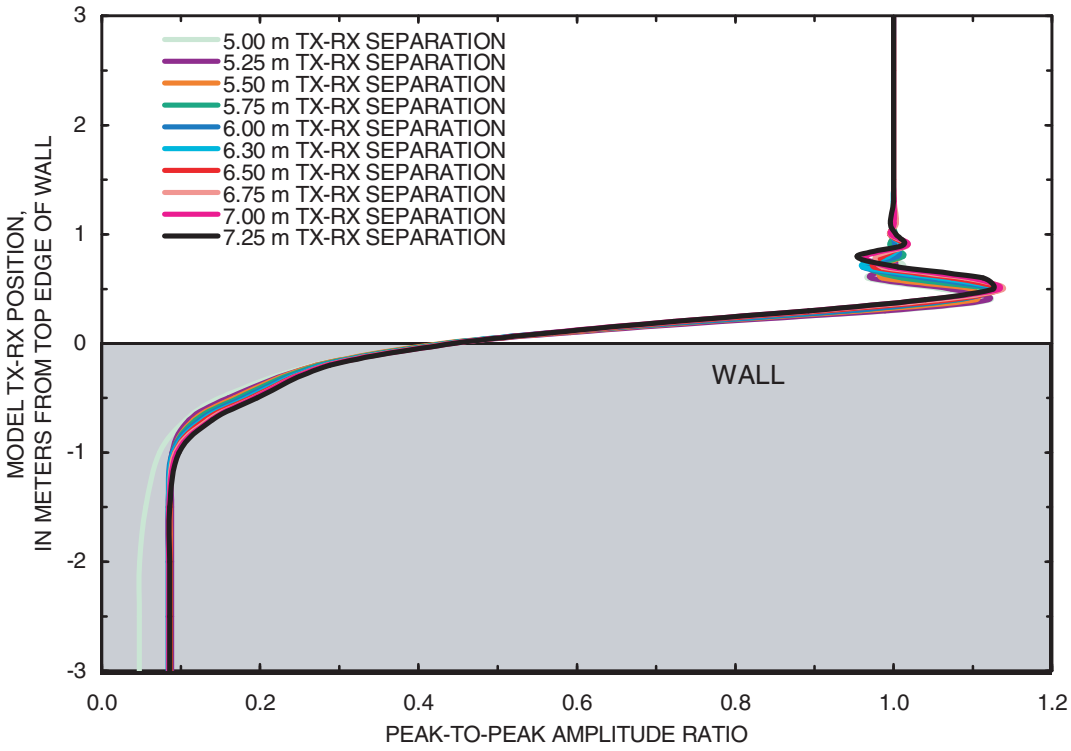

Figure 3. Model amplitudes, normalized to background amplitudes, for transmitter (TX) - receiver (RX) separations ranging from 5.00 to 7.25 meters plotted from 3.0 meters above top edge to 3.0 meters below top edge of the wall.

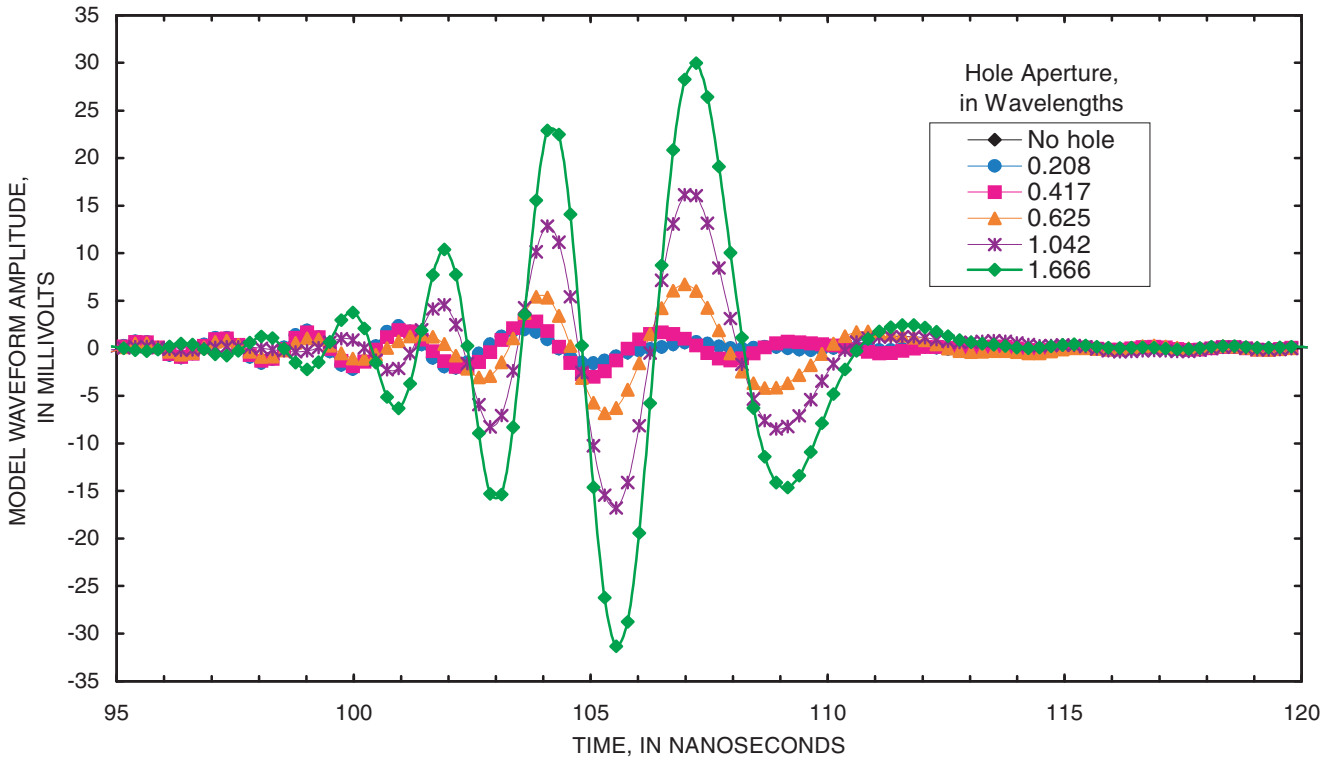

Figure 4. Model waveforms for transmitter - receiver separation of 6.30 meters in hole apertures ranging from 0 to 1.67 wavelengths (0 to 40 centimeters).

Physical Modeling

The numerical-modeling results were compared to radar data obtained from laboratory-scale physical models designed to simulate the geometry and dimensions of the numerical models relative to the wavelength of the transmitted pulse. Scaled physical modeling was conducted at the Aldridge Geophysical Imaging Laboratory at Columbia University. The laboratory-scale physical model was constructed from an ordinary aquarium with interior dimensions of 119.4 cm by 43.4 cm by 75.0 cm (fig. 5). The aquarium was filled with sand saturated with water. A perfect conductor was simulated by wrapping aluminum foil around a cardboard template. Two Malå GeoScience RAMAC antennas with approximate center frequencies in air of 900 MHz were used as the transmitter and receiver. Radar-transmission data were acquired by moving the transmitting and receiving antennas, positioned on opposite sides of the tank, across the 119.4-cm-long horizontal axis of the tank in 1-cm increments. Radar traces were recorded at 55,828 MHz using 1,024 samples per trace.

To determine background transmitted pulse amplitudes and wavelengths, measurements were made across the tank containing only saturated sand. The average wavelength of the transmitted pulse in the saturated sand of the laboratory tank was 5.5 cm, with an average amplitude of about 40,000 microvolts. Measurements also were made with a continuous aluminum foil template placed along the long axis of the tank to test the assumption that the aluminum foil would simulate a perfect conductor and prevent the penetration of the radar pulse across the tank. With the continuous aluminum foil template placed in the tank, the pulse amplitude was about 0.1 percent of the background pulse amplitude, indicating that the aluminum sheet was a perfect conductor in this physical model.

In the model designed to determine the effect of the wall edges on the radar direct-wave amplitude, the aluminum foil template extended across one-half of the tank (fig. 5); while in the model designed to determine the effect of holes, the template extended across the entire length of the tank

[1] The use of trade names in this report is for identification purposes only and does not constitute an endorsement by the U.S. Geological Survey

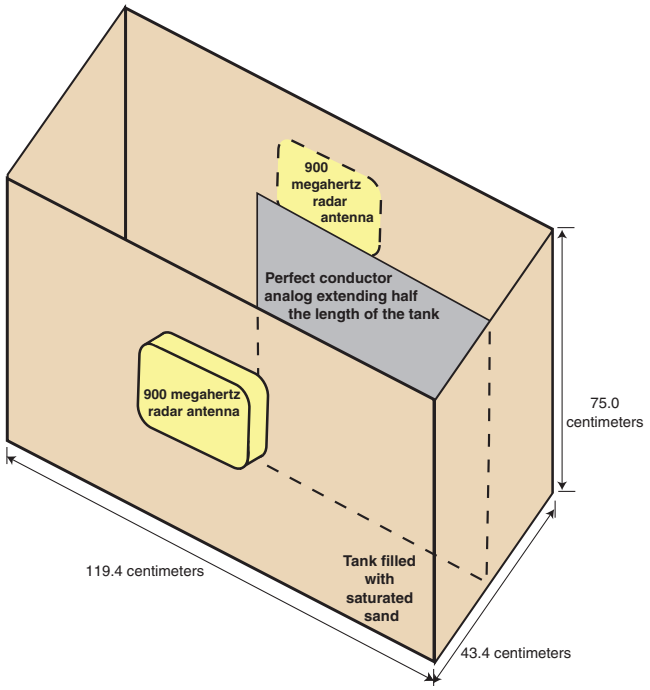

Figure 5. Physical model with a perfect conductor, simulating the iron wall, extending half of the length of the tank.

with a hole in the center; hole aperture varied between 0.36 and 2.00 wavelengths (2 and 11 cm) (fig. 6). These models were designed as physical analogs to the field-scale problems simulated by the numerical models.

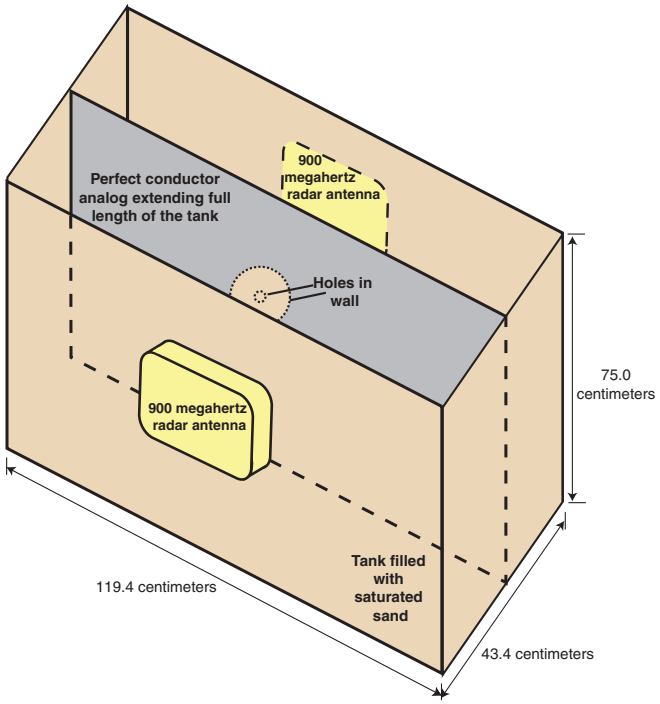

Figure 6. Physical model with a perfect conductor, simulating the iron wall, extending the length of the tank and with of hole apertures 0.36 and 2.00 wavelengths in the center.

Cross-tank radar pulse amplitudes from the half-wall physical model are shown plotted against antenna position in figure 7. Pulse amplitudes from the physical model have been normalized to the average background pulse amplitude. The physical-model data are shown juxtaposed to the numerical-model results for the case of a borehole separation of 5 m. The transmitted pulse amplitude decreases as the antenna positions approaches the edge of the aluminum model wall. The edge of the aluminum sheets correlates with the position of the scan where the transmitted pulse amplitude decreases to about 0.41 of the normalized background pulse amplitude (fig. 7). The behavior of transmitted pulse amplitude with respect to conductor edges observed in the physical model correlates closely with the results of the 2-D FDTD modeling, where the position of the wall edge corresponds to a decrease in normalized radar-pulse amplitude of about 0.43.

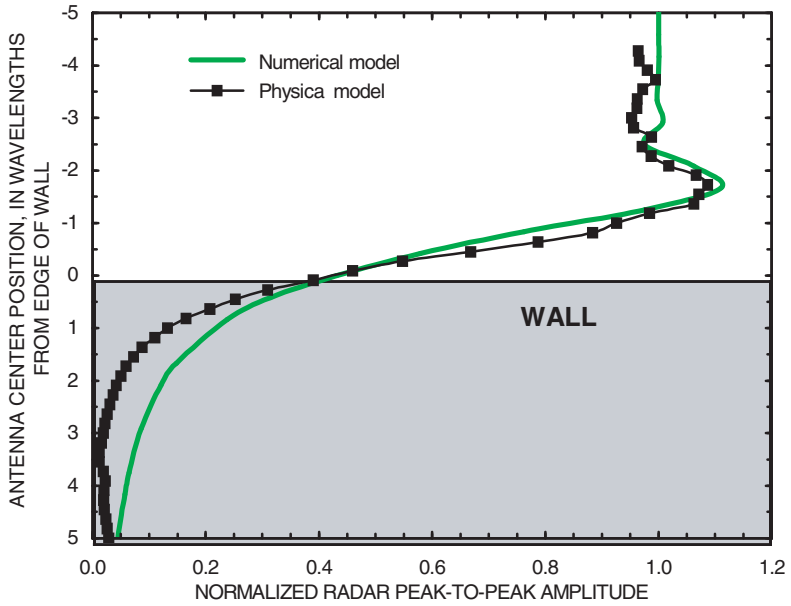

Figure 7. Half-wall physical model radar data overlain with half-wall numerical data with an antenna separation of 5.00 meters.

Cross-tank radar-pulse amplitudes from the hole-in-wall model plotted against distance from the center of the hole are shown in figure 8. Pulse amplitudes from the physical model have been normalized to the average background pulse amplitude. The radar direct-pulse amplitudes increase with the increase in the aperture of the hole. The normalized radar direct-pulse amplitude would not have detected the 0.36 wavelength hole, but would have detected the 2.0 wavelength hole. The results of the physical modeling are qualitatively consistent with the results of the numerical modeling, but there are not enough hole-in-wall physical modeling data to determine the limits of hole detection.

The correlation between the amplitude trends predicted by the 2-D FDTD numerical modeling and the amplitude trends observed in radar data acquired from the physical wall-edge and hole-in-wall models indicate that the numerical models can be used to interpret amplitude trends observed in cross-hole radar field data.

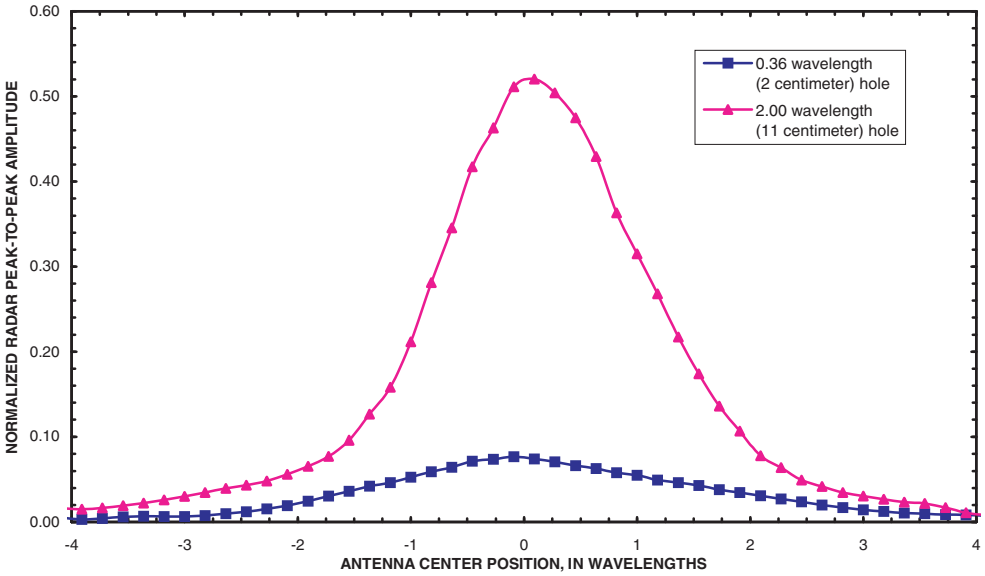

Figure 8. Normalized peak-to-peak amplitudes for waves transmitted in the hole-in-wall physical model through the perfect conductor analog for holes of 0.36 and 2.00 wavelengths (2 and 11 centimeters).

Collection, Processing, and Analysis of Geophysical Data

Conventional geophysical logging and cross-hole radar scanning were conducted at the field site before and after iron injection. The conventional logs included electromagnetic (EM)- induction and borehole deviation.

Twenty-six observation boreholes were installed at the field site. Of these, 20 were used for this study (fig. 9). The boreholes were drilled to depth of about 46 m, and were completed with 7.62-cm diameter PVC. Five of the boreholes were damaged or destroyed during the wall installation

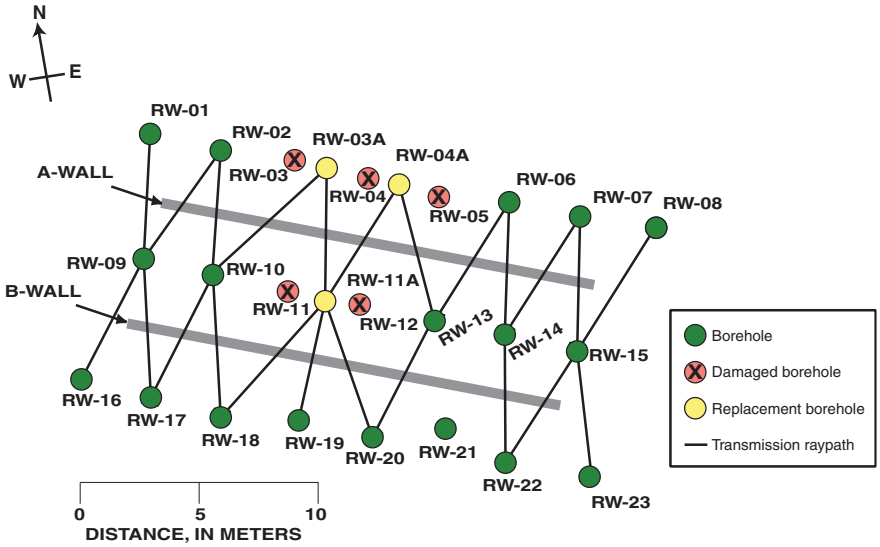

Figure 9. Map view of the observation boreholes with transmission raypaths. The damaged boreholes were deformed during the iron wall installation, and were unusable for radar data collection. The replacement boreholes were drilled after the iron injection to replace the damaged boreholes.

procedure and could not be used. Three replacement boreholes were installed after the wall installation to permit acquisition of radar data in the area of the damaged boreholes.

Cross-hole Radar Scanning

Cross-hole radar field data were acquired with a Malå GeoScience RAMAC[1] borehole-radar system using electric-dipole antennas with center frequencies in air of about 100 and 250 MHz. Radar scans were conducted in 20 observation boreholes located in three rows parallel to the injection zones (fig. 9). A radar scan of the region between two boreholes was constructed from cross-hole measurements acquired by moving a radar transmitter and receiver in unison at 10-cm increments from the top of the casing to the bottom of the borehole. At each antenna position, 32 traces were stacked and recorded using a sampling frequency of 2,635 MHz and 1,024 samples per trace.

Processing of the cross-hole radar data was limited to band-pass filtering to reduce random noise. After filtering, the peak-to-peak amplitude of the direct wave from each trace was measured. Under the assumption that iron was not introduced into sediments below a depth of 40 m, the amplitudes measured for each well-pair were normalized relative to the average amplitude of "normal" cross-hole measurements below 40 m depth. Thus, a normalized value near 1.00 indicates that the pulse amplitude is close to the background level.

Based on the numerical and physical modeling results, the following method was used to analyze the field data: (1) locations where post-injection amplitudes decreased to 0.43 of the normal pulse amplitude were interpreted as a wall edge (fig. 3); (2) locations where normalized amplitudes were below 43 percent and were bounded by wall edges were interpreted as a continuous wall zone; and (3) locations where normalized amplitudes exceeded 0.43 and were within a wall zone were interpreted as discontinuities (holes) in a section of wall.

The normalized amplitude data were combined into cross sections and contoured. Normalized amplitude data below the 0.43 contour are shown for the A and B walls (fig. 10). For the A wall (fig. 10a) the contouring outlines two irregularly shaped low-amplitude areas; one extends about 12 m horizontally and 6.5 m vertically from about 24.5 to 31 m below land surface, and another zone extends

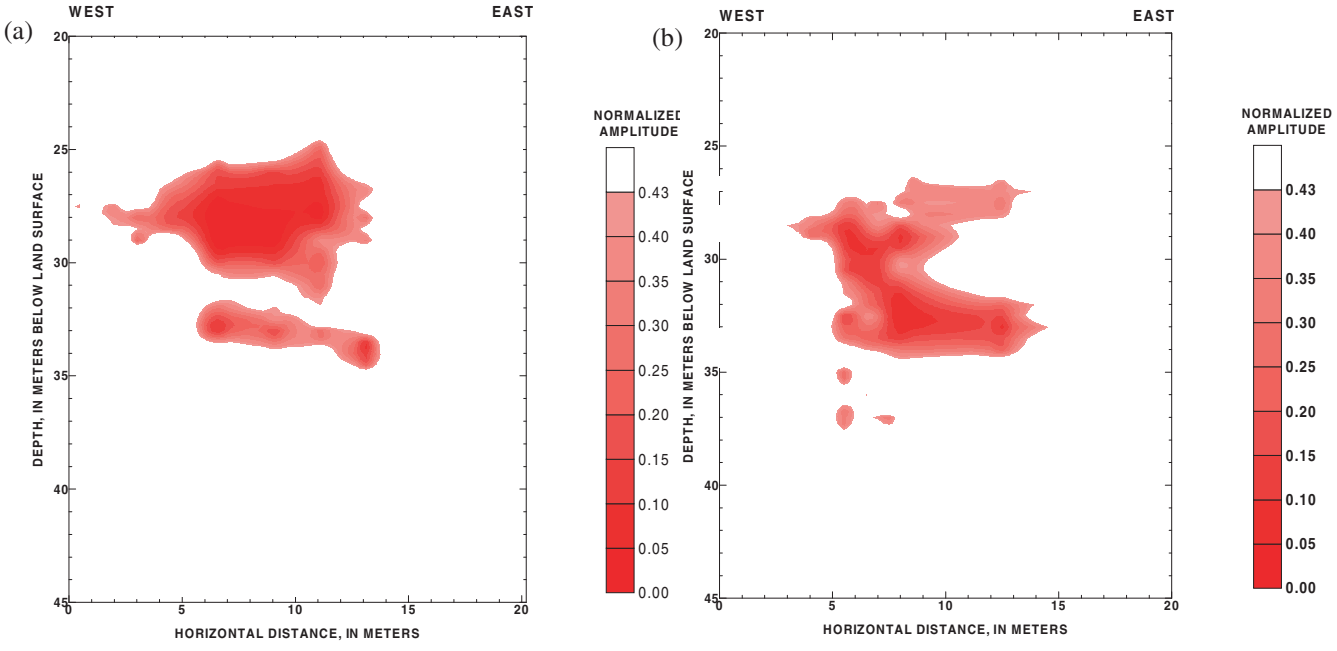

Figure 10. Post-injection direct-wave amplitudes across the (a) A-wall and (b) B-wall showing normalized amplitudes of less than 0.43.

about 8 m horizontally and 2.5 m vertically from about 32 to 34.5 m. For the B wall (fig. 10b) the contouring outlines a large, irregularly shaped low-amplitude area that extends about 8 m horizontally and 7 m vertically from about 27 to 34 m below land surface. These continuous low-amplitude areas are interpreted as zones of iron wall.

Based on the numerical and physical modeling results, no observations of either the A or B walls indicated the presence of holes in the wall zones. This indicates that (1) iron in wall zones is distributed in a generally continuous manner; (2) holes, if any, exist at scales smaller than the resolution limit of the radar antennas and acquisition geometry used for this study; and/or (3) irregularities in iron distribution are such that holes in one area are masked by accumulations of iron in other areas.

Single-Hole Radar Reflection Scanning

To determine if single-hole radar reflection methods could be used to image the wall, data were collected in boreholes RW-01 to RW-08 and RW-16 to RW-23 before, after, and, in some boreholes, during the installation of the wall. The data were acquired with a Malå GeoScience RAMAC[1] borehole-radar system using electric-dipole antennas with center frequencies in air of about 100 and 250 MHz. At each antenna position, 32 traces were stacked and recorded using a sampling frequency of 1,811 MHz and 1,024 samples per trace.

The data collected during and after the wall installation were differenced from the background data to minimize the reflections from geologic features and boreholes. The difference in reflection data between the background data and data collected during the wall installation in RW-04 is shown in figure 11. A distinct reflector can be seen at a depth of 32 m and is interpreted as the leading edge of the iron movement toward RW-04. A reflection from a near-horizontal feature intercepts the borehole at a depth of about 27 m. This is interpreted as a thin layer of iron that flowed away from the main body of the wall through a permeable layer and entered the borehole. The iron injection mix was found in the top of the antenna cable head, and the mix was later pulled from the well with a bailer. RW-04

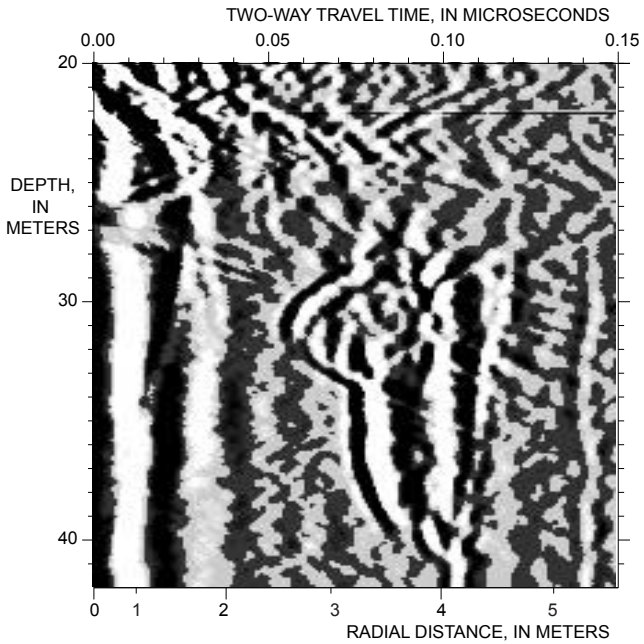

Figure 11. 100-megahertz borehole radar reflection data from borehole RW-04 differenced between background and data collected during the wall installation.

was impassable after the iron injection was completed.

The single-hole reflection data were also processed using migration techniques in order to estimate the position of the iron walls. The migration was done using a constant velocity, two-dimensional Kirchhoff migration (Yilmaz, 1987), which migrates each sample to a circle in the image plane. The image plane is defined as the horizontal plane that intersects the borehole at the transmitter and receiver measuring point. This is a simplification that can be justified because the energy associated with reflections from high angles will be low compared to the reflection energy associated with low angles due to the radiation patterns of the antennas.

Before to the migration of the reflection data, the known positions of the boreholes were used to filter the data to remove reflections from other boreholes. After the filtering had been performed, the reflection from the iron wall was identified, and all other data were muted out, thus reducing the noise in the migrated image. The data were migrated, resulting in a circular distribution of energy in three dimensions. By examining the lateral and temporal amplitude and correlation of this energy, the probable location of the wall was determined and identified the relative strength of the reflection from the wall. The migrated wall reflection data from boreholes RW-17 and RW-18 are shown in figure 12. The envelope of the migration circles corresponds with the known approximate position of the iron wall.

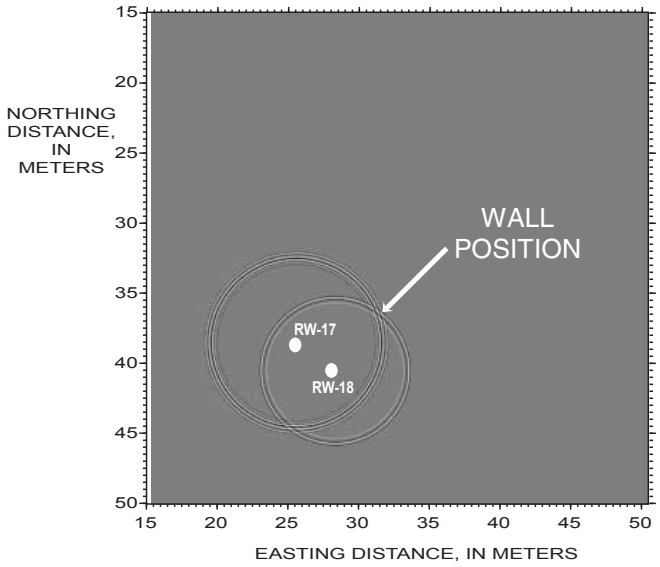

Figure 12. Migrated borehole radar reflection data from boreholes RW-17 and RW-18 imaged at a depth of 30 meters.

A full three-dimensional migration, taking angle dependent amplitude information into account, coupled with a spatial filter is planned. This should enhance the results of the reflection data processing and improve the ability to image the wall in three dimensions.

Summary

A pilot-scale study was conducted at the Massachusetts Military Reservation, Cape Cod, Massachusetts, to assess the use of a hydraulic fracturing method to create vertical, permeable walls of zero-valent iron to remediate ground water contaminated by chlorinated solvents. Contamination exists at depths that exceed the practical construction limits of conventional iron walls. The study was conducted near the source area of a chlorinated solvents plume where ground water is contaminated

from 24 to 37 m below land surface. A treatment zone was designed for the study, which consisted of two parallel reactive-iron walls 12 m long, 13 m high, and 0.15 m thick, and which were separated by about 6.1 m, and designed to intersect and remediate a portion of the plume.

Results from numerical and physical modeling were used to interpret the radar-wave amplitude data. The numerical and physical models consist of saturated sand containing a wall of perfectly conducting material. Results from both models show that the amplitude of a transmitted radar pulse crossing the edge of a conductive wall is about 43 percent of the amplitude of a radar pulse transmitted through background material. The modeling results indicate that holes in the wall with a diameter of less than 40 percent of the wavelength of the radar pulse are not likely to be detected.

The U.S. Geological Survey used a cross-hole common-depth radar scanning method to estimate the lateral and vertical extent and continuity of the two walls emplaced with the hydraulic-fracturing method. The cross-hole radar survey used boreholes installed on opposite sides of the two iron injection zones. Based on the results of the numerical and physical modeling, the radar field data indicate that iron in the A-wall is distributed in two zones: the upper zone is about 12 m wide, extending from 24.5 to 31 m below land surface, and the lower zone is about 8 m wide, extending from about 32 to 34.5 m below land surface. The iron in the B-wall is distributed in a generally continuous zone about 8 m wide, extending from about 27 to 34 m below land surface. No discontinuities are interpreted to be present within the boundaries of either the A- or B-wall zones. As part of a feasibility study, single-hole radar reflection data were collected and successfully used to image the surface of the wall. The use of a three-dimensional migration technique, coupled with a spatial filter, will probably enhance the results of the reflection data processing.

Acknowledgments

The authors thank the U.S. Air Force Center for Environmental Excellence at the Massachusetts Military Reservation, Edward L. Pesce, Rose Forbes, Michael Minior, and the U.S. Army National Guard for their support. The authors gratefully acknowledge David Hubble of the University of Waterloo for his assistance before, during, and after the iron installation. The authors acknowledge the staff of Golder Sierra LLC for their assistance during the iron installation. The authors gratefully acknowledge Lei Xiao and Dr. Lanbo Liu of the University of Connecticut for the use of the finite-difference model and Justin Kuczynski of the Aldridge Geophysical Imaging Laboratory of Lamont-Doherty Earth Observatory at Columbia University for his assistance with the physical modeling.

References

ABB Environmental Services, Inc., 1993, Task 2-5C remedial investigation field sampling and analysis plan, priority one areas of contamination: January 1993, various pagination.

Gillham, R.W. and O'Hannesin, S.F. (1994), "Enhanced degradation of halogenated aliphatics by zero-valent iron", *Ground Water*, v. 32, no. 6, pp. 958-967.

Hubble, D.W. and Gillham, R.W. (1997), "Work plan for deep emplacement of granular iron PRW by vertical hydrofracturing and slurry injection – demonstration at CS-10 source area plume Massachusetts Military Reservation", University of Waterloo, Ontario, various pagination.

Hubble, D.W. and Gillham, R.W. (1999), "Installation of deep reactive walls at MMR using a granular iron-guar slurry", *U.S. Geological Survey Toxic Substances Hydrology Program-Proceedings of the Technical Meeting, Charleston, South Carolina March 8-12, 1999, Water Resources Investigations Report 99-4018C,* v. 3, pp. 431-438.

Ricker, N. (1953), "The form and laws of propagation of seismic wavelets", *Geophysics*, v. 18, pp. 10-40.

Smyth, D.J.A., Shikaze, S.G., and Cherry, J.A. (1996), "Hydraulic performance of permeable barriers for in situ treatment of contaminated groundwater", *Assessment of barrier containment technologies, a comprehensive treatment for environmental remediation applications*, Springfield, Virginia, pp. 881-886.

Starr, R.C., and Cherry, J.A. (1994), "In situ remediation of contaminated ground water-- the funnel-and-gate system", *Ground Water*, v. 32, no. 3, pp. 465-476.

Xiao, Lei; Liu, Lanbo; and Cormier, V.F. (1998), "Two-dimensional finite-difference time-domain solution for Maxwell's equations using pseudo-spectral method", *Proceedings of the Seventh International Conference on Ground Penetrating Radar (GPR'98*), Lawrence, Kansas, May 27-30, 1998, Lawrence, Kansas, pp. 585-589.

Yilmaz, Özdoðan (1987), Seismic Data Processing, Tulsa, Oklahoma, pp. 241-353.